Single- and two-phase heat transfer in tangential injection-induced swirl flow

Z. Guo and V. K. Dhir
Mechanical, Aerospace and Nuclear Engineering Department, School of Engineering and Applied Science, University of California, Los Angeles, Los Angeles, CA, USA

Single- and two-phase heat transfer in a vertical flow with tangential injection was investigated in this work. The tubular test section was electrically heated, and distilled water was used as the working fluid. The test sections had a length of 110.0 cm and a diameter of 1.727 cm. Heat transfer coefficients were measured over a length of up to 46.5 cm. In the experiments, total mass flux was varied from 640 kg/m^2·s to 2500 kg/m^2·s, and water inlet temperature was between 23° and 75°C. The system pressure was 3.07 bar.

With tangential injection, up to fourfold increase in average heat transfer coefficient has been observed for single-phase flow in the range of experimental parameters studied. The heat transfer coefficient is found to increase to a very large value just downstream of the injection location, and then it decreases nearly exponentially with distance. Injector angles of 70° and 90° with the tube axis were studied. In the experiments either two or four injectors placed at one location were operational. The heat transfer coefficients are correlated with the ratio of the tangential and axial momentum of the flow. Under subcooled boiling conditions, the heat transfer enhancement due to injection is smaller than that in single-phase flow. It is found that with swirl a larger superheat is required to initiate boiling. Under fully developed boiling conditions, the swirl has little effect on the heat transfer coefficient, but there can be significant enhancement in critical heat flux (CHF).

Keywords: convection; single and two phase; swirl; boiling; tangential injection

Introduction

Economic and energy considerations continuously motivate investigators to search for efficient methods of energy transfer. For a given heat exchanger, enhancement in heat transfer coefficients can lead to an increase in the rating of the heat exchanger. Or for a given heat load, the reduction in overall resistance can lead to a smaller heat exchanger. In other applications, efficient heat removal may be desirable to prevent excessive temperatures or even equipment damage when a certain amount of energy is to be dissipated over a limited area. Swirl flow is one of the techniques that has been used successfully in the past to augment heat transfer.

According to Bergles and Webb,[1] about 250 publications on swirl flows had been cited by the end of 1983. Among them, about 140 articles were related to single-phase convective heat transfer. Most of the swirl flows were created by insertion of a twisted tape in the tube. Twisted tapes, when inserted into tubes, tend to promote turbulence as well as to intensify mixing of the hot and cold fluids. This in turn improves the heat transfer process. The enhancement is generally higher in laminar flows than in turbulent flows. Unfortunately, enhancement in heat transfer coefficient is always accompanied by an increase in the pumping power. Among the reported data on heat transfer augmentation, the data of Junkhan *et al.*[2] are typical. In their experiments, turbulators type A and B, consisting of narrow, thin metal strips bent and twisted in a zigzag fashion, displayed respective increases of 135% and 175% in heat transfer coefficient at a Reynolds number of 10,000. Turbulator type C, consisting of a twisted strip with width slightly less than the tube diameter, provided a 65% increase in heat transfer coefficient. However, the corresponding friction factor increases in the three cases were 1110%, 1000%, and 160% respectively. Their results also showed a decrease in heat transfer enhancement as the Reynolds number was increased.

Another technique of enhancing heat transfer is the use of vertical flow. A detailed description of this kind of flow and its potential in heat transfer enhancement were given by Razgaitis and Holman.[3] According to them, one promising technique for the augmentation of convective heat transfer is the use of confined swirl flows, particularly of the decaying vortex type. Vortical flow is distinguished by a significant circulation-preserving region; this flow type arises when a flow with some initial angular momentum is allowed to decay along the tube axis. A flow with vorticity has the characteristics of the entry-length region, since fully developed flow implies the absence of tangential velocity.

As also suggested by Kreith and Margolis,[4] swirl flow can be created by tangentially injecting part of the fluid along the axis of the flow channel, thereby leading to enhancement in heat transfer. But they did not carry out any experimental effort to support their suggestion. Tauscher *et al.*[5] claimed that their work represented the first attempt to augment heat transfer coefficients by injecting the same fluid to the main stream flow. However, in their work fluid was injected radially, and the flow did not have any tangential component. Recently, Weede and Dhir,[6] for the first time, have successfully used tangential injection induced swirl flow to enhance critical heat flux in subcooled flow boiling. In another work, Dhir and Scott[7] studied the superposition of multilocation injection induced swirl flow on enhancement of subcooled critical heat flux.

The purpose of the present work is to explore some aspects of single- and two-phase heat transfer in the injection-created swirl flow.

Address reprint requests to Prof. V. K. Dhir at the Mechanical, Aerospace and Nuclear Engineering Department, University of California, Los Angeles, Los Angeles, CA 90024-1597, USA.

Received 10 October 1988; accepted 21 December 1988

Experimental apparatus and procedure

Apparatus

The flow loop used for this study is shown schematically in Figure 1. The system consists of a centrifugal pump, a turbine flowmeter, a bank of visual flowmeters, a test section, two pressure transducers, and a heat exchanger. Two storage tanks were used for adjusting fluid temperature. Distilled water was circulated with a pump which gave a flow rate of 4.5 m^3/hr at a discharge pressure of 70 bar. Part of the flow was bypassed, and flow to the test section was divided into two parts: one for injection and the other for straight flow through the test section entrance.

The test section was ohmically heated with current provided from a 100-kW DC power supply. One of the test sections used in the experiments is shown in Figure 2. The tube material was Inconel 600 alloy, cold-drawn annealed-redrawn, with a 1.727-cm I.D. and a 0.089-cm wall thickness. The total length of the test section was 110.0 cm, and heat transfer coefficient was measured over a length of up to 46.5 cm. Two copper terminals were mounted to connect the power supply to the test section. A hydrodynamic entry length of 23 diameters was allowed upstream of the injection location. The injectors were situated 2.5 cm downstream of the first electrode.

Details of an injector design are also shown in Figure 2. A 2.54-cm-diameter, 1.0-cm-wide brass ring was silver soldered to the test section. Two or four holes were milled tangentially, 180° or 90° apart, at a 70° angle to the tube axis. The injectors were made of 0.386 cm I.D., 1.2-cm-long stainless steel tubes. They were machined such that the end had the same curvature as the inside of the test section surface and were silver soldered to the brass ring. A nozzle with a pressure tap was soldered to each injector.

The inlet and outlet water temperatures and test section surface temperatures were monitored using 30 gage Chromel-Alumel thermocouples. Thermocouples on the test section surface were employed at selected axial locations, with two thermocouples placed 30° apart at each location. To protect the test section from damage, one of the thermocouples just upstream of the second electrode was connected to a temperature controller for automatic shutoff of the power supply in case

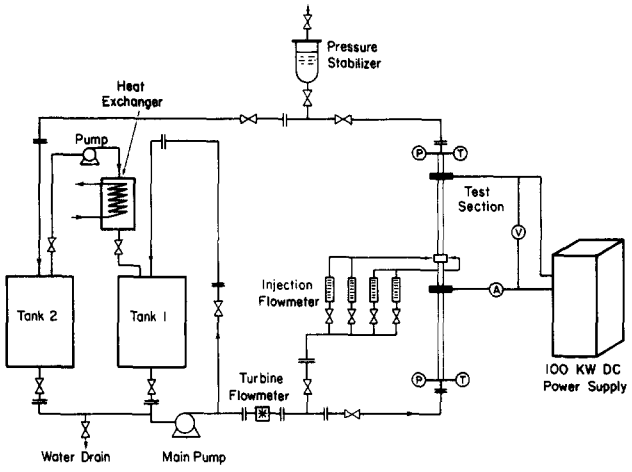

Figure 1 Schematic diagram of the flow loop

Notation

C, C_1, C_2	Constants
D	Internal diameter of the test section
d_j	Internal diameter of the injectors
E	Net heat transfer enhancement on constant pumping power basis
f	Friction factor
h	Heat transfer coefficient
h_{fg}	Latent heat of vaporization
L	Total length of the test section over which heat transfer coefficients were measured
$\dot{m}_j$	Mass flow rate of the injected fluid
$\dot{m}_T$	Total mass flow rate at the test section exit
M_j	Momentum of the injected fluid; $\dot{m}_j^2/\pi d_j^2 \rho_l/4$
M_t	Tangential momentum of the injected fluid, $M_j \sin\theta$
M_T	Total momentum of the axial flow, $\dot{m}_T^2/\pi D^2 \rho_l/4$
N_j	Number of injectors operational at one location
Nu	Local Nusselt number as observed in the experiments
Nu_0	Nusselt number in fully developed flow as predicted from correlations
Nu_{fd}	Nusselt number in fully developed flow as observed in the experiments
Nu_s^*	Normalized local Nusselt number in swirl flow: Nu_s/Nu_0
$\overline{Nu_s^*}$	Normalized average Nusselt number as defined in Equation 7
$\overline{\overline{Nu_s^*}}$	Normalized average Nusselt number as defined in Equation 8
Pr	Prandtl number of liquid
q	Heat flux based on test section inside surface area
$(r_c)_{max, min}$	Maximum and minimum cavity sizes given by Equation 14
R	Test section radius
Re	Reynolds number based on total flow rate
S	Swirl number, $\int_0^R \rho u v r^2\, dr / R \int_0^R \rho u^2 r\, dr$
T_b	Local bulk liquid temperature as calculated from heat balance
T_s	Saturation temperature corresponding to system pressure
T_w	Test section inside wall temperature
u	Axial velocity component in swirl flow
v	Tangential velocity component in swirl flow
V_a	Average axial liquid velocity in purely axial flow
V_s	Average axial liquid velocity in swirl flow
z_j	Axial distance from injection location

Greek symbols

β	Contact angle
δ	Thickness of the thermal layer
ε_1	Ratio of average heat transfer coefficient in a modified flow to that in purely axial flow
ε_2	Ratio of pumping power consumed in a modified flow to that in a tube without flow modification
θ	Angle extended by injector to the tube axis
μ_b	Viscosity of liquid at local bulk temperature
μ_w	Viscosity of liquid at local wall temperature
ρ_l	Density of liquid
ρ_v	Density of vapor
σ	Surface tension of liquid
Ψ	Net heat transfer enhancement

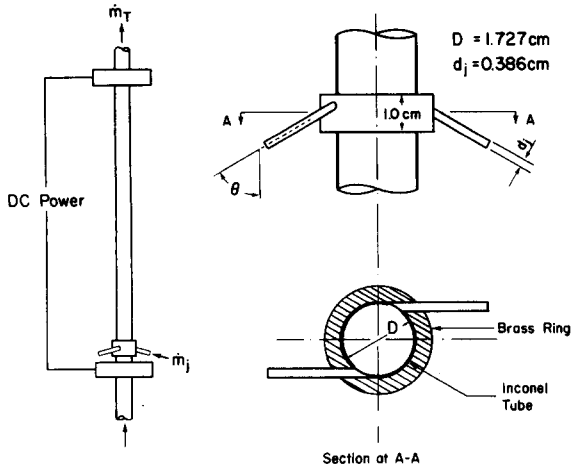

Figure 2 Test section and the details of injectors

CHF should occur. The thermocouples used for tube wall temperature measurement were electrically insulated from the wall by placing a very thin sheet of mica between the thermocouple hot junctions and the tube surface. To prevent heat loss by convection and radiation, the outside surface of the test section was covered with 6-cm-thick fiberglass insulation material protected by an aluminum foil. Calibration tests showed that the error in heat transfer coefficient due to heat loss was negligible.

All temperature data and DC current and voltage drop over the test section were recorded on a Fluke 2280A data logger. The inlet and outlet pressure of the test section, pressure difference over the heated section, and the pressure difference between injector inlet and heated section outlet were measured with an Omega PX302 and Omega PX820 transducers. The total flow rate through the test section was measured with a Flow Technology turbine flowmeter FT-16N50-LB and an electronic frequency counter for digital readout of the frequency. The flow rate through each injector was obtained with a bank of Dwyer VFB "Visi-Float" variable-area flowmeters.

Procedure

Prior to an experimental run, the secondary pump was used to circulate water through the heat exchanger to adjust the fluid temperature. Thereafter, the main pump was started and the flow rate and pressure were set to the desired level. Subsequently the amount of injection was adjusted. The total flow rate, which included the flow through the test section entrance and that through the injectors, was kept constant in each test. After the power supply was switched on, the power applied to the test section was adjusted to a desired level by changing the input voltage.

In two-phase heat transfer experiments, power to the test section was increased in steps. Between consecutive steps enough time was allowed for the wall temperature to reach steady state before a data point was taken. Heat flux was increased until CHF conditions were reached.

Data reduction

Local heat transfer coefficients were calculated from the definition $h=q/(T_w-T_b)$. The ohmic heat generation rate was assumed to be uniform because of the weak dependence of electrical resistivity of Inconel 600 alloy on temperature. However, the thermal conductivity of Inconel 600 alloy is a strong function of temperature. Its functional dependence on temperature was obtained from the work of Hogan.[8] To calculate the inside tube wall temperature from the measured outside wall temperature, the one-dimensional steady-state heat conduction equation with variable thermal conductivity was solved numerically. Heat conduction in the axial direction was neglected, since the test section wall was relatively thin. Local liquid bulk temperature was calculated from heat balance. The overall uncertainty in the single-phase heat transfer coefficients is calculated to be $\pm 5.2\%$.

Results and discussion

Single- and two-phase flow heat transfer coefficients were obtained under both axial and swirl conditions. In this work swirl intensity is expressed as the ratio of the tangential momentum at the injection location and the axial momentum of the total flow and is written as

$$\frac{M_t}{M_T}=\frac{M_j}{M_T}\sin\theta=\left(\frac{\dot{m}_j}{\dot{m}_T}\right)^2\left(\frac{d_j}{D}\right)^2\frac{\sin\theta}{N_j} \tag{1}$$

where N_j is the number of injectors operational and $\dot{m}_j$ and $\dot{m}_T$ are the total mass flow rates through the injectors and at the test section exit, respectively. The momentum ratio as defined in Equation 1 is related to the swirl number S, commonly used in the literature as

$$S=\frac{M_t}{M_T}\frac{\int_0^R r^2uv\,\mathrm{d}r}{R\int_0^R ruv\,\mathrm{d}r} \tag{2}$$

where u and v are the axial and tangential velocity components of the flow, respectively. In the experiments the momentum ratio was varied over a range of 0 to about 10. Data were obtained with water mass velocities varying from 640 to 2500 $\mathrm{kg/m^2\cdot s}$.

In presenting the experimental results, a normalized Nusselt number is defined as

$$\mathrm{Nu}^*=\frac{\mathrm{Nu}}{\mathrm{Nu}_0} \tag{3}$$

where Nu is the experimentally determined Nusselt number and Nu_0 is the Nusselt number in fully developed axial flow as calculated from appropriate correlations based on local flow conditions. It is deemed important to compare the experimentally determined fully developed Nusselt number Nu_{fd} in purely axial flow with the correlations. Axial flow heat transfer data were recorded in every test before swirl flow was applied. The asymptotic value of Nusselt number in each such test was taken to be the fully developed value. The experimental results were compared with the correlation recommended by Petukhov:[9]

$$\mathrm{Nu}_0=\frac{(f/8)\,\mathrm{Re}\,\mathrm{Pr}}{1.07+12.7\sqrt{f/8}(\mathrm{Pr}^{2/3}-1)}\left(\frac{\mu_b}{\mu_w}\right)^n \tag{4}$$

where $n=0.11$ for $T_w>T_b$ and f is the friction factor which for smooth tubes is given as

$$f=\frac{1}{(1.82\log_{10}(\mathrm{Re})-1.64)^2} \tag{5}$$

It was found that 90% of the data were within $\pm 7\%$ of the correlation.

Single-phase forced convection with swirl

Experimentally determined heat transfer results with injector angle of 70° and two injectors operational at one location are

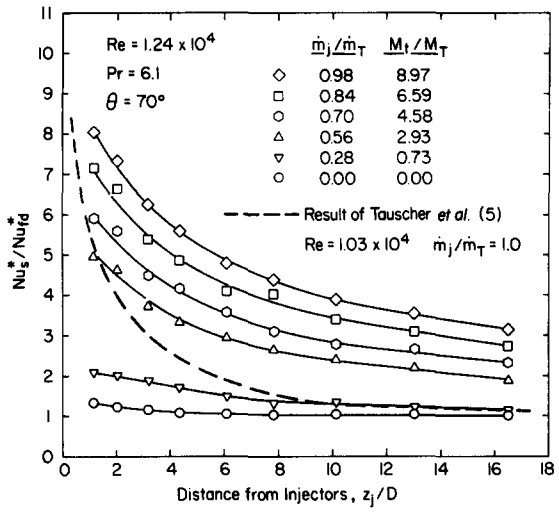

Figure 3 Ratio of normalized Nusselt number in swirl flow to that in fully developed purely axial flow as a function of axial distance

plotted in Figure 3. The ordinate represents the ratio of normalized Nusselt number with swirl, Nu_s^*, to the normalized Nusselt number for thermally fully developed flow in the absence of swirl, Nu_{fd}^*. The abscissa represents axial distance in hydraulic diameters from the injection location. The figure shows that the heat transfer data with swirl appear to resemble a hydrodynamically and thermally developing flow. However, for a fixed total flow rate the increase in heat transfer coefficient at a given location is found to strongly depend on the momentum ratio, M_t/M_T. The magnitude of heat transfer in swirl flow is much larger than the one observed in the thermally developing region of a purely axial flow. This enhancement in heat transfer is basically due to the thinning of thermal and hydrodynamic boundary layers when a tangential velocity component superimposes on the axial flow. An increase in local velocity with tangential injection can also intensify the flow turbulence.

In the reported data, centripetal acceleration induced secondary flow is not believed to be responsible for enhancement in heat transfer coefficient. An experiment conducted with a momentum ratio of 4.4 and a temperature difference as high as 120°C between the tube wall and the bulk liquid showed no appreciable change in heat transfer coefficient after variation in viscosity with temperature was accounted for. The observation is consistent with what has been reported earlier by Kuo *et al.*[10] for rotating flow heat transfer with water.

In Figure 3 the dotted line shows the result of Tauscher, Sparrow, and Lloyd[5] obtained by injection of water normal to the main flow of the same fluid. Their results shown here are for the case when all of the fluid was injected radially. Those data should be compared to the present data with $\dot{m}_j/\dot{m}_T = 0.98$. With radial injection, flow separation and reattachment occurred immediately downstream of the injection location. In the absence of the tangential velocity component, the effect of injection appears to die down very rapidly after reattachment. With introduction of swirl, a centripetal force is created in the flow field. Under this condition, boundary layer separation is not possible. Local heat transfer decreases along the tube axis as the tangential momentum is lost because of viscous dissipation and fluid mixing. In comparison to radial injection, heat transfer enhancement with tangential injection is sustained for a much longer distance.

The heat transfer data for Reynolds numbers of 2.38×10^4 and 3.40×10^4 are compared in Figure 4. In both cases the injectors made an angle of 90° with the tube axis. It is seen that flow Reynolds number has little effect on the increase in heat transfer with swirl. In Figure 5, the ratio of normalized local Nusselt number with swirl to that for fully developed purely axial flow is plotted as a function of axial distance for Prandtl numbers of 6.0 and 4.0. The flow Reynolds number in both cases was 2.38×10^4. It is seen that with smaller Prandtl number the rate of heat transfer with swirl is slightly higher. A qualitative explanation for this behavior can be obtained by noting the role played by Prandtl number in a developing flow. For a fluid with $Pr > 1$, the thermal layer is thinner than the hydrodynamic layer, whereas the reverse is true for a fluid with $Pr < 1$. Since the presence of swirl limits the thickness as well as the growth of the hydrodynamic boundary layer, the effect of swirl is larger when the thermal layer has a tendency to protrude out of the hydrodynamic boundary layer.

For $2.3 < Pr < 6.3$ and $1.2 \times 10^4 < Re < 6.0 \times 10^4$, more than 90% of the data are correlated within $\pm 10\%$ by

$$\frac{Nu_s^*}{Nu_{fd}^*} = 1 + 0.48e^{-0.4(z_j/D)} + 2.3\left(\frac{M_t}{M_T}\right)^{0.68} e^{-0.22(z_j/D)^{0.56}Pr^{0.25}} \tag{6}$$

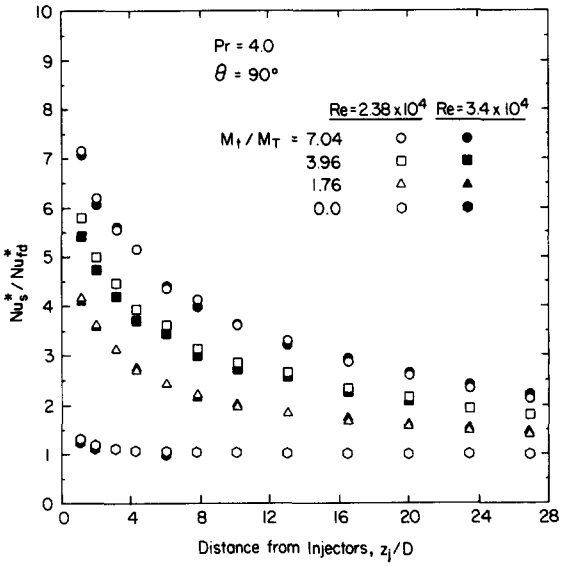

Figure 4 Effect of Reynolds number on heat transfer enhancement

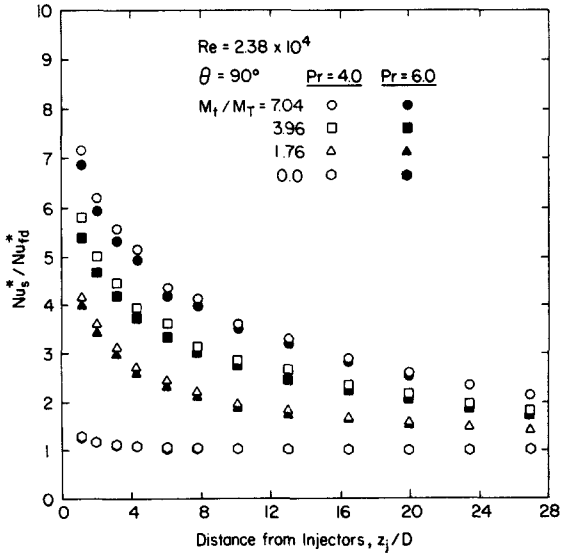

Figure 5 Effect of Nusselt number on heat transfer enhancement

where the first two terms on the right-hand side represent a developing axial flow. Swirl flow effect on heat transfer enhancement is expressed by the third term. In the developing axial flow, the effect of Prandtl number in the exponentially decaying term is not explicitly included. This does not impose a large error in the calculated value since in the experiments the Prandtl number was varied over a narrow range. In Equation 6, Prandtl number is based on the fluid temperature at entrance. It should also be noted that Equation 6 is based on data covering a very limited range of Prandtl number. A larger data base covering a wide range of Prandtl number is needed to fully substantiate the functional dependence on Prandtl number.

From a practical point of view, it is more convenient to use average Nusselt number. In such a case, the normalized average Nusselt number is defined as

$$\overline{\mathrm{Nu}_s^*}=\frac{1}{z_j/D}\int_0^{z_j/D}\mathrm{Nu}_s^*\,\mathrm{d}\left(\frac{z_j}{D}\right) \tag{7}$$

The results corresponding to the data plotted in Figure 3 are shown in Figure 6. In this figure, the heat transfer coefficients obtained by Molki and Sparrow[11] for hydraulically and thermally developing axial flow are also plotted. In swirl flow both the hydrodynamic and thermal boundary layers are destroyed upon injection. A comparison of the decay of the heat transfer coefficients in swirl flow with that in a purely axial flow clearly shows that boundary layer reconstruction mechanisms are different for the two flows. Heat transfer coefficients decay much slower in swirl flow than they do in the developing region of a purely axial flow.

Normalized Nusselt number averaged over the whole length over which heat transfer coefficients were measured is

$$\overline{\overline{\mathrm{Nu}_s^*}}=\frac{1}{L/D}\int_0^{L/D}\mathrm{Nu}_s^*\,\mathrm{d}\left(\frac{z_j}{D}\right) \tag{8}$$

and the heat transfer enhancement due to swirl is defined as

$$\Psi=\frac{\overline{\overline{\mathrm{Nu}_s^*}}}{\mathrm{Nu}_{fd}^*}-1 \tag{9}$$

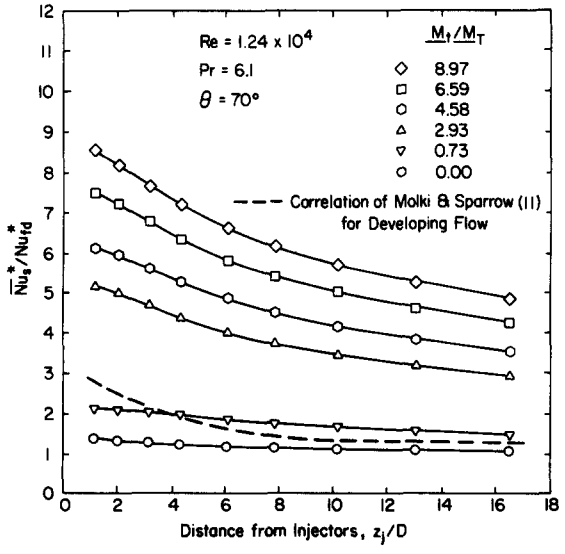

Figure 6 Ratio of normalized average Nusselt number in swirl flow to that in fully developed purely axial flow as a function of axial distance

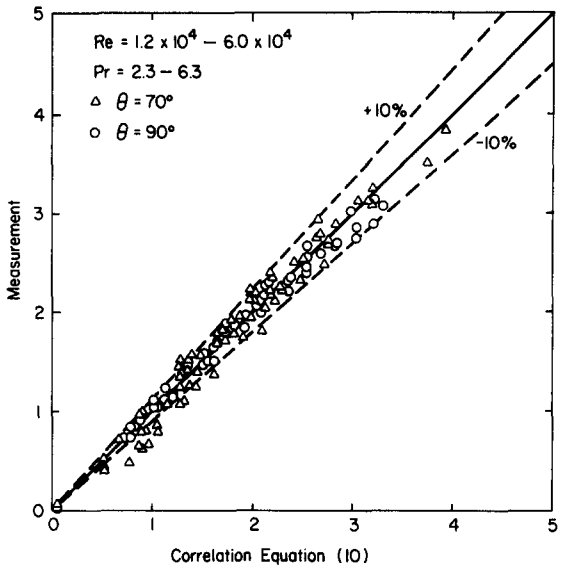

Figure 7 Comparison of prediction from Equation 10 and measurement

Integration of Equation 6 yields an expression for enhancement as

$$\Psi=\frac{1.2}{L/D}\left(1-e^{-0.4(L/D)}\right)+\frac{2.3}{L/D}\left(\frac{M_t}{M_T}\right)^{0.68}\int_0^{L/D}e^{-0.22(z_j/D)^{0.56}\mathrm{Pr}^{0.25}}\,\mathrm{d}\left(\frac{z_j}{D}\right) \tag{10}$$

The calculations from Equation 10 are compared with the experimental measurements in Figure 7. This figure includes results for Reynolds number between 1.2×10^4 and 6.0×10^4, Prandtl number between 2.3 and 6.3, and injector angles of 70° and 90°. Figure 7 shows that more than 95% of the data are correlated with Equation 10 within $\pm10\%$. It should be kept in mind that the first term on the right-hand side of Equation 10 is due to the thermal entry-length effect and includes the influence of tube wall imperfection at the injector section on axial flow. The contribution of this term to the overall heat transfer enhancement becomes small for large M_t/M_T and large L/D. For very short tubes Equation 10 will give values which are optimistic in terms of enhancement due to swirl.

The results and correlations presented so far are for swirl flow with two injectors operational at one location. Tests with four injectors at one axial location were also conducted. For this case the test section was fabricated following the same procedure as described before, and the injection angle was 70°. The only difference is that the injectors were now 90° apart, equally spaced along the tube circumference. Figure 8 shows a comparison of the heat transfer data obtained in two injector tests and four injector tests with a momentum ratio of 2.42. It can be seen that with four injectors the heat transfer coefficient decays at a slightly slower rate and has a lower value near the injection location than that obtained with two injectors. However, the average heat transfer enhancement in both cases still correlates well with Equation 10.

In any heat transfer enhancement technique, the penalty in terms of the pumping power is an important concern. Thus a rational comparison of different heat transfer enhancement techniques can only be made on a constant pumping power basis. If fully developed turbulent flow in a smooth pipe is used for normalization, an expression for net heat transfer enhancement on a constant pumping power basis can be derived.

The friction factor of turbulent flow in a smooth tube can

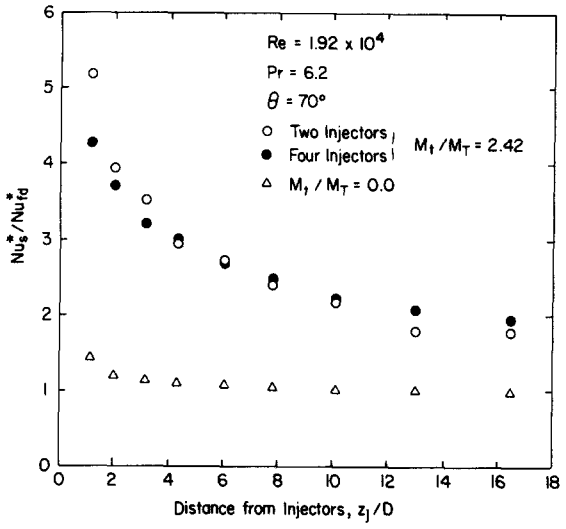

Figure 8 Comparison of heat transfer enhancement with two injectors and that with four injectors

be approximated as

$$f=\frac{C}{\mathrm{Re}^{0.25}} \qquad 3\times10^3\le\mathrm{Re}\le10^5 \tag{11}$$

whereas the Nusselt number for fully developed flow is proportional to $\mathrm{Re}^{0.8}$. When the flow is modified to enhance heat transfer, it is usually accompanied by an increase in friction factor. In injection induced swirl flow injectors contribute significantly to the total pressure loss. This pressure loss can be distributed over the tube length to calculate the effective friction factor. Equating the pumping power in a smooth tube with that for the modified configuration, the ratio of velocities in the modified to the axial flow is

$$\frac{V_s}{V_a}=\frac{1}{\varepsilon_2^{1/2.75}} \tag{12}$$

where ε_2 is the ratio of the friction factors in the modified flow and that in axial flow in smooth tubes. Defining, for a given velocity, the ratio of the average heat transfer coefficient in the modified configuration to that for purely axial flow in a smooth tube by ε_1, one can write the net enhancement in heat transfer as

$$E=\frac{\varepsilon_1}{\varepsilon_2^{0.8/2.75}}-1=\frac{\varepsilon_1}{\varepsilon_2^{0.29}}-1 \tag{13}$$

In the present technique the pumping power is lost in the injectors as well as in the main tube. The measurements of pressure drop in the injectors as well as the fittings connecting the injectors to the flow lines gave a loss factor of unity. Within the uncertainty of the measurements the friction factor, when all of the fluid was injected tangentially, was found to be three to four times that for purely tangential flow. The known pressure loss in the injectors and in the tube was used to evaluate ε_2 for the present method.

Equation 10 is applied to compare the swirl flow results with those from the three types of inserts studied by Junkhan *et al.*[2] Heat transfer results in swirl flow, with 90° injector angle and four injectors operational, were averaged over a length of 26.9 tube diameters. The swirl flow had a Prandtl number of 4.0 and the flow with inserts had a Prandtl number of 0.7. It is found that each method has quite different characteristics with respect to Reynolds number. At a Reynolds number of 1.5×10^4, when 25% of the fluid is injected tangentially, the swirl flow yields a net enhancement of 20.2% and flow with inserts of type A, B, and C give a net enhancement of 21.7%, 8.0%, and 14.8%, respectively. At a Reynolds number of 3.0×10^4, net enhancement with 20% injection is 15%, while the three types of inserts give enhancements of 6.8%, 6.8%, and −5.3%, respectively. Swirl flow with fluid injection becomes superior to all three types of inserts at high Reynolds numbers. Since the experimental results showed that injection-induced swirl flow is more effective in heat transfer enhancement in low-Prandtl-number fluids, a larger enhancement would be calculated if a Prandtl number of 0.7 is used. In addition, injection-induced swirl flow has the flexibility that the ratio of the injected flow rate to the total flow rate can be adjusted easily to give the optimal performance according to the heat load requirement.

It should be noted here that in the present injector design injected fluid passed through a tubular section. Most of the pumping power was consumed in the injection section. This design can be modified to reduce the injection pressure drop and further improve the overall benefit of injection-induced swirl flow.

Boiling inception and partial boiling

The observed heat transfer coefficients as a function of axial distance from the injection location are plotted in Figure 9 for several wall heat fluxes. In the single-phase flow region, the heat transfer coefficients decrease with distance from the injection location. With the increase in heat flux, the onset of nucleation signals an improvement in the rate of heat transfer. As a result, a minimum in the heat transfer coefficient–versus–distance curve is observed. This minimum approximately represents the boiling inception boundary and is shown as a broken line in Figure 9. The exit of the heated section is the location where nucleation occurs first. This is due to the fact that at exit the swirl intensity is the lowest while the liquid enthalpy is the maximum. As the heat flux is increased, the boiling front moves toward the injection location. Eventually, the single-phase region is limited to the immediate vicinity of the injectors.

Figures 10 and 11 show the heat flux as a function of wall superheats for axial locations of $z_j/D=6.1$ and $z_j/D=13.0$, respectively. These figures include data for both axial and swirl flows. Using the boiling nucleation criterion developed by Hsu,[12] the range of cavities that can nucleate at a given superheat is

$$(r_c)_{\max,\min}=\frac{C_1\delta}{2C_2}\left(\frac{T_w-T_s}{T_w-T_b}\right)\left\{1\pm\sqrt{1-\frac{8C_2\sigma T_s(T_w-T_b)}{\delta\rho_v h_{fg}(T_w-T_s)^2}}\right\} \tag{14}$$

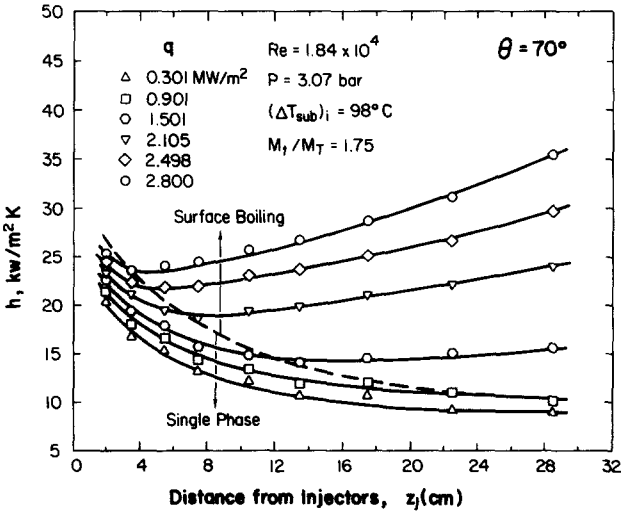

Figure 9 Inception of boiling under swirl flow conditions

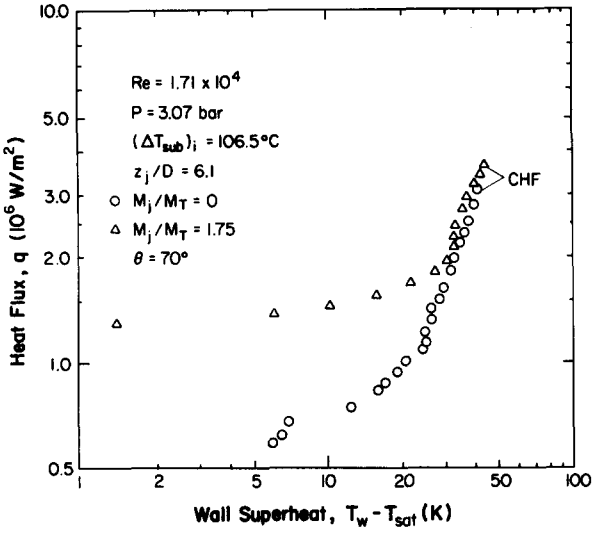

Figure 10 Comparison of heat flux versus wall superheat in swirl flow and purely axial flow at $z_j/D=6.1$

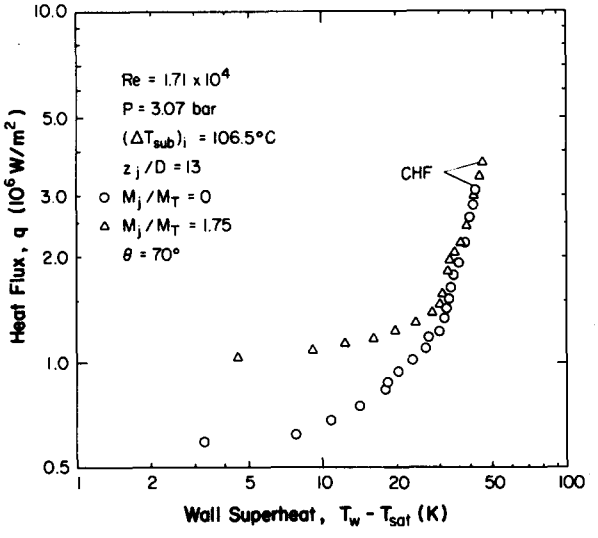

Figure 11 Comparison of heat flux versus wall superheat in swirl flow and purely axial flow at $z_j/D=13.0$

In the above equations, the constants C_1 and C_2 depend on contact angle. The functional dependence of these constants on contact angle for a spherical bubble embryo is

$$C_1=\sin\beta \qquad C_2=1+\cos\beta \tag{15}$$

In the present analysis, a contact angle of 90° is assumed, so both constants have a value of unity. At $z_j/D=6.1$, boiling inception under purely axial flow conditions is found to occur at a wall superheat of 7.0°C. For this superheat, Equation 14 gives the range of active cavity size as 2.7 to 4.8 μm.

The minimum superheat for nucleation as obtained from Equation 14 by setting the term under the square root sign equal to zero is found to be 6.5°C. The corresponding cavity size is 3.5 μm. Thus experimentally observed nucleation superheat is very close to the predicted minimum superheat. Table 1 lists results of similar calculations for both axial and swirl flows at $z_j/D=6.1$ and 13.0. The important inference that can be drawn from Table 1 is that swirl does not alter the inception characteristics, except that nucleation with swirl occurs at a higher superheat. This is due to thinning of the thermal layer. The inception heat flux calculated from the correlation developed by Bergles and Rohsenow[13] is found for purely axial flow to be 7.7×10^5 W/m^2 and 7.3×10^5 W/m^2 at $z_j/D=6.1$ and $z_j/D=13.0$, respectively. The heat flux values for the swirl flow are 1.64×10^6 W/m^2 and 1.20×10^6 W/m^2. The corresponding superheats for axial flow are 12.6 and 12.3°C and those for swirl flow are 18.0 and 15.5°C.

It is interesting to note in Figures 10 and 11 the existence of a slight overshoot just prior to the development of fully developed nucleate boiling in flows with and without swirl. Calculations similar to those described above indicate the nucleation of cavities with radius 0.3 to 0.4 μm at the observed superheats. It is possible that a large number of such cavities are present on the surface as a result of the process (cold-drawn annealed-redrawn) used in the manufacture of the test section tubing. A sudden nucleation of such cavities results in the observed behavior.

Fully developed boiling

When the nucleation process is fully developed, the boiling activity entirely dominates the heat removal from the wall, and the convective process plays a secondary role. As a result in fully developed boiling, the heat transfer coefficients with and without swirl have nearly the same value. This is clearly seen in Figure 11 for wall superheat greater than 41°C. A similar result was observed by Lopina and Bergles[14] in tape-generated swirl flow. The fully developed boiling heat flux varies with wall superheat as $(T_w-T_s)^{4.2}$. This is consistent with what was reported by McAdams *et al.*[15] and Jens and Lottes[16] for subcooled boiling in vertical tubes. All of the data obtained at $z_j/D=6.1$ in swirl flow appear to correspond to partially developed boiling. Finally, it should be mentioned that although heat transfer coefficients in fully developed nucleate boiling have the same value for both swirl and axial flows, the critical heat fluxes with swirl can be much higher, as has been shown by Weede and Dhir.[6] This is confirmed by the present study.

Conclusions

(1) Enhancement in single-phase heat transfer coefficients occurs when the same fluid is injected tangentially along the tube

Table 1 Comparison of predicted and measured wall superheats and cavity sizes at inception of nuclear boiling

Flow z_j/D	Without swirl		With swirl	
	6.1	13.0	6.1	13.0
Heat flux at boiling incipience, 10^6 W/m^2	0.64	0.64	1.51	1.11
Observed wall superheat, °C	7.0	8.0	10.2	9.4
Cavity size corresponding to observed heat flux, μm	2.7–4.8	1.7–7.4	1.5–3.6	1.5–4.7
Predicted minimum wall superheat, °C	6.5	6.5	9.9	8.5
Cavity size corresponding to minimum wall superheat, μm	3.5	3.5	2.3	2.6

axis. More than 700% increase in local heat transfer coefficient has been observed when all of the fluid is injected tangentially.

(2) Single-phase heat transfer coefficients in injection-induced swirl flow decrease along the tube length but at a much smaller rate than that for a purely axial developing flow.

(3) It is found that the enhancement of average heat transfer coefficients in swirl flow is a function of the tangential to total flow momentum ratio. In the range of parameters studied the enhancement is found to be insensitive to flow Reynolds number but is weakly affected by fluid Prandtl number.

(4) On a constant pumping power basis, heat transfer enhancement by injection-induced swirl flow is found to be superior to flow with tube inserts especially for Reynolds number greater than 1.7×10^4.

(5) In fully developed boiling, no influence of swirl on boiling heat transfer coefficient is observed. However, the critical heat flux with swirl can be much higher than that for a purely axial flow.

Acknowledgments

The authors wish to acknowledge the support of the Division of Engineering and Geosciences, Office of Basic Energy Sciences, U.S. Department of Energy under grant No. DE-FG03-85ER13360 and the Gas Research Institute under contract No. 5086-260-1535.

References

1 Bergles, A. E. and Webb, R. L. A guide to the literature on convective heat transfer augmentation. *Advances in Enhanced Heat Transfer*, 1985, HTD **43**, 81–89

2 Junkhan, G. H., Bergles, A. E., Nirmalan, V., and Ravigarurajan, T. Investigation of turbulentors for fire tube boilers. *J. Heat Transfer*, 1985, **107**, 354–360

3 Razgaitis, R. and Holman, J. P. A survey of heat transfer in confined swirl flow. *Heat and Mass Trans. Processes*, 1976, **2**, 831–866

4 Kreith, F. and Margolis, D. Heat transfer in turbulent vortex flow. *Applied Science Research, Sec. A*, 1959, **8**, 457–473

5 Tauscher, W. A., Sparrow, E. M., and Lloyd, J. R. Amplification of heat transfer by local injection of fluid into a turbulent tube flow. *Int. J. Heat Mass Transfer*, 1970, **13**, 681–688

6 Weede, J. and Dhir, V. K. Experimental study of the enhancement of critical heat flux using tangential flow injection. *Fundamentals of Heat Transfer in Fusion Systems*, 1983, HTD **24**, 11–18

7 Dhir, V. K. and Scott, J. H. On the superposition of injection induced swirl flow during enhancement of subcooled critical heat flux. *Int. J. Heat Mass Transfer*, 1987, **30**, 2013–2022

8 Hogan, C. L. The thermal conductivity of metals at high temperature. Ph.D. Dissertation, Lehigh University, 1950

9 Petukhov, B. S. Heat transfer and friction in turbulent pipe flow with variable physical properties. In *Advances in Heat Transfer*, Vol. 6, Academic Press, 1970, 504–564

10 Kuo, C. Y., Iida, H. T.,Taylor, J. H., and Kreith, F. Heat transfer in flow through rotating ducts. *J. Heat Transfer*, 1960, **82**, 139–151

11 Molki, M. and Sparrow, E. M. An empirical correlation for the average heat transfer coefficient in circular tubes. *J. Heat Transfer*, 1986, **108**, 482–484

12 Hsu, Y. Y. On the size of range of active nucleate cavities on a heating surface. *J. Heat Transfer*, 1962, **84** C(3), 207–216

13 Bergles, A. E. and Rohsenow, W. M. The determination of forced-convection surface-boiling heat transfer. *J. Heat Transfer*, 1964, **86**, 365–372

14 Lopina, R. F. and Bergles, A. E. Subcooled boiling of water in tape-generated swirl flow. *J. Heat Transfer*, 1973, **95**, 281–283

15 McAdams, W. H., Kennel, W. E., Minden, C. S. L., Carl, R., Picornel, P. M., and Dew, J. E. Heat transfer at high rates to water with surface boiling. *Ind. Engng. Chem.*, 1949, **41**(9), 1945–1953

16 Jens, W. H. and Lottes, P. A. Analysis of heat transfer burnout, pressure drop and density data for high pressure water. *ANL-4627*, May 1951